

The equilibrium melting temperature of *cis*-polyisoprene

E. N. Dalal, K. D. Taylor and P. J. Phillips*

Department of Materials Science and Engineering, University of Utah, Salt Lake City, Utah 84112, USA

(Received 9 November 1982; revised 10 February 1983)

The equilibrium melting temperature T_m of *cis*-polyisoprene (*Hevea* natural rubber) has been determined to be 35.5°C at atmospheric pressure. The optical 'turbidimetric' technique developed to obtain the melting data, discussed in this paper, utilized unpolarized light and was free of complications (presumably involving melt strain) encountered with polarized light techniques, but was found to be consistent with that and other techniques. The effect of variables such as heating rate and crystallization time were considered. Two independent methods of extrapolation of the T_m data to evaluate T_m° produced values in the range $T_m^\circ = 35.5^\circ \pm 0.3^\circ\text{C}$. The fold surface free energy σ_e was also estimated, by two independent methods, to be 0.024 J m⁻².

Keywords Polyisoprene; rubber; melting; thickening; equilibrium; crystal

INTRODUCTION

It is well known that the melting point of a polymer is dependent on the lamellar thickness because of the very small values of that dimension normally encountered. Melting points are usually extrapolated in one of several possible manners in order to predict the equilibrium melting temperature, which is the melting point of an infinitely thick crystal¹. The two most common procedures are (a) to use a plot of melting temperature *versus* crystallization temperature and to extrapolate to the temperature where the two are equal, and (b) to use a direct plot of melting temperature *versus* reciprocal lamellar thickness. Both approaches are fraught with problems arising from (a) accurate measurement of the melting point, (b) crystal thickening during crystallization and (c) crystal thickening as the melting point is approached during the melting experiment.

cis-Polyisoprene is a relatively slowly crystallizing polymer which exhibits lamellar thickness in the range 5–10 nm and minor thickening compared to many other polymers. Studies are complicated somewhat by the high supercoolings necessary for crystallization (typically 40°–80°C)². It does have the advantage, however, that the lamellar thicknesses can easily be measured using transmission electron microscopy of stained samples and hence the lamellar thickness–supercooling relation is well established. The best value of the equilibrium melting point currently available is 39°C obtained using dilatometry by Kim and Mandelkern³. This value was determined, in essence, not by the extrapolation of the melting point of the dominant α -crystals^{2,3}, which would be preferred, but by using, in the main, occasionally ill-defined points of inflection which were ascribed to the melting of β -crystals. α -Crystals could not be used for the primary extrapolation since the relation between melting temperature and crystallization temperature was grossly non-linear. In this communication we wish to report the results of a new extensive investigation of the melting behaviour of *cis*-

polyisoprene which has resulted in an accurate measurement of the equilibrium melting point of α -crystals.

EXPERIMENTAL

cis-Polyisoprene in the form of pale crepe was supplied by MRPRA, Brickendonbury, Herts, UK, and was Soxhlet extracted to remove soluble additives, such as stearic acid, prior to use. A number of specimens were also studied after the gel fraction was removed; however, corroborative studies showed that the presence of gel did not significantly affect the results.

Specimens were prepared by putting a small amount of processed *cis*-polyisoprene between a microscope slide and a cover glass, and pressing at 130°C in a hydraulic press for about 40 s. Spacers were used to control thickness, with best results obtained with a thickness of about 0.2 mm.

The specimens were melted in a Mettler FP52 microfurnace whose temperature was controlled by a Mettler FP5 control unit. This unit provides accurate temperature control ($\pm 0.1^\circ\text{C}$ static) and can heat or cool at rates from 0.2° to 10°C min⁻¹. The microfurnace was mounted on a Reichert transmitted-light microscope fitted with a photosensor connected to a Metrologic photometer, whose analogue output was recorded on a strip chart recorder. Sub-ambient temperatures (down to -20°C) were achieved by blowing a stream of nitrogen gas, cooled in liquid nitrogen, through a port provided on the microfurnace. Condensation on the microfurnace windows at these low temperatures was avoided by placing the assembly in a glove-box purged with dry nitrogen. Light level perturbations due to line fluctuations were minimized by the use of a constant-voltage transformer.

Before each experiment, the specimens were heated to 70°C for 30 min under vacuum to nullify the effects of previous crystallization. They were then put into miniature polyethylene envelopes which were purged with dry nitrogen and individually heat-sealed with a commercial sealing device. Sets of such sealed specimens were crystallized at the desired temperature in a Neslab refrigerated

* To whom all correspondence should be addressed

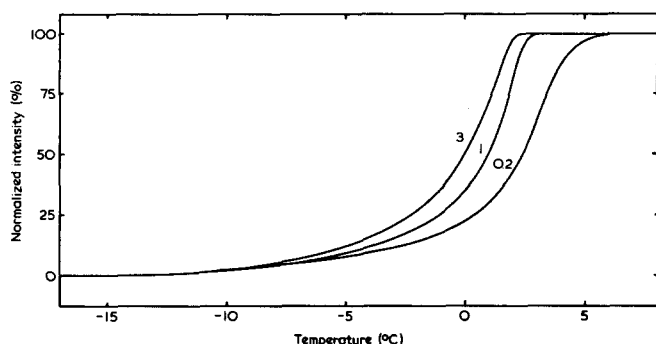


Figure 1 Typical 'turbidimetric' melting traces from the chart recorder showing the effect of heating rate ($^{\circ}\text{C min}^{-1}$) on the melting trace. All samples crystallized at -15°C for 24 h

bath filled with a 40 wt% ethylene glycol solution. After the specimen was allowed to crystallize for a predetermined time, the envelope was slit and the slide rapidly (~ 1 s) inserted into the FP52 stage which had been precooled to the crystallization temperature. The specimen was then melted at the prescribed heating rate, with continuous transmitted-light recording as described earlier.

Thermal lag in the specimen was investigated by inserting a thermocouple into one of the specimens. The lag was found to be approximately proportional to the heating rate, and the proportionality constant was estimated to be ~ 0.3 min. This value was used to correct the results for thermal lag.

Preliminary experiments indicated that a complication developed when standard polarized light techniques were used, in the form of a large peak in transmitted-light intensity at or very near the melting point. The height of this peak clearly increased with crystallization time, ranging from virtually zero at the shortest times to an order of magnitude larger than the intensity at maximum crystallinity at the longest times used. The exact temperature location of this peak was apparently somewhat random, and independent of heating rate. This peak posed a serious problem by obscuring the actual melting trace at all except the lowest crystallization times. The peak might possibly represent a photoelastic effect associated with melt strain.

A 'turbidimetric' approach, using unpolarized light, was completely free of this effect at all crystallization times. This technique depends on the reduction of transmitted-light intensity by light scattering from the crystals. It is therefore sensitive to the melting of entire spherulites and not to the early melting of less stable crystals produced by, say, infilling mechanisms of previously rejected material. The light level in a melting trace increases sharply on melting (see Figure 1). Melting points determined by unpolarized and polarized light techniques at short crystallization times were identical.

Melting data obtained by this turbidimetric technique have been compared⁴ with those from differential scanning calorimetry (d.s.c.) and wide-angle X-ray scattering (WAXS), and found to produce melting temperatures within 0.5°C of those obtained by the d.s.c. and WAXS techniques. However, on comparison with the WAXS melting curves it was evident that the turbidimetric transmitted-light intensity is distinctly non-linear with crystallinity, being much more sensitive to low crystalline levels and saturating relatively rapidly.

D.s.c. endotherms clearly showed the low-temperature peak noted by Kim and Mandelkern³ and attributed to ' β '-crystals². This peak corresponds to a barely perceptible bump on the dilatometric melting curve³. The corresponding perturbation on the WAXS curves was also unclear, whilst the turbidimetric curves showed no trace of this effect, presumably due to the β -lamellae occurring predominantly as infilling lamellae and not as individual spherulites. Consequently, all of the melting data obtained by this technique apply only to the ' α '-crystals.

The effect of gel content was studied in an auxiliary experiment in which a 1% cis-polyisoprene solution was run through a coarse filter and then through a $1.2 \mu\text{m}$ g.f.c. filter. The polymer collected on each of these filters, as well as the filtrate, was precipitated with methanol, washed and dried, then pressed into specimens as described earlier. Under identical conditions, these specimens and unfiltered specimens produced melting traces that were indistinguishable within experimental scatter. This result was anticipated from the work of Kim and Mandelkern³, who found that the melting temperature was essentially independent of gel content.

DEFINITION OF MELTING TEMPERATURE

The first problem encountered in analysing the melting data is in defining a melting temperature from the transmitted-light intensity trace. Some possible definitions are shown schematically in Figure 2. The return-to-baseline definition $T_{m,B}$ is quite commonly used, and corresponds to the highest observed melting temperature in the distribution. It is, however, a poor choice for several reasons.

The $T_{m,B}$ definition is strongly dependent on the detector sensitivity⁵. The trace approaches the amorphous baseline asymptotically at an extremely low angle, and so a very small shift along the intensity axis corresponds to a relatively large shift along the temperature axis. For the same reason, small uncertainties in defining the baseline (due to noise) lead to large uncertainties in

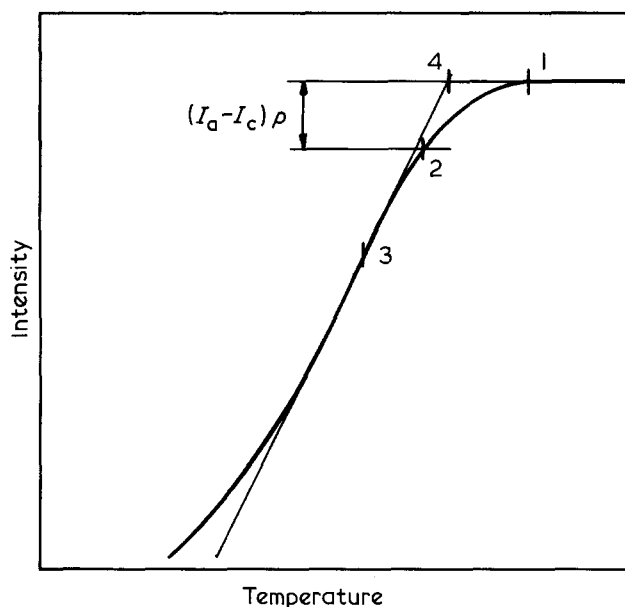


Figure 2 Possible definitions of melting temperature from a melting trace: 1, baseline; 2, residual crystallinity ρ ; 3, maximum slope; 4, extrapolated

$T_{m,B}$. Since increased sensitivity is almost invariably accompanied by increased noise, $T_{m,B}$ is certain to be poorly defined.

Another major disadvantage of $T_{m,B}$ involves the thickening effect (due to melt recrystallization and/or accelerated thickening just below the melting point) inevitable when melting a polymer at a finite heating rate. Since $T_{m,B}$ represents the highest observable melting temperature, it is obviously strongly influenced by this thickening effect, particularly when studying thinner crystals. It can also produce excessively high values of the melting temperature due to superheating or due to thermal gradients within large specimens.

An alternative definition⁵ is the temperature $T_{m,p}$ at which a specified (small) fraction p of the original crystals remains. This cannot be used here directly because of the non-linear response, but an equivalent definition for small values of p in the case of a transmitted-light intensity trace would be the intersection of the trace with a line corresponding to the normalized intensity

$$(I - I_c)/(I_a - I_c) = 1 - p$$

where I is the transmitted-light intensity and the subscripts 'c' and 'a' refer to the limiting values at the beginning and end of the melting experiment. If p is very small, $T_{m,p}$ is subject to the same errors as $T_{m,B}$; in fact, $T_{m,B}$ is a special case of $T_{m,p}$ with $p=0$. On the other hand, Weeks⁵ has pointed out that large values of p are susceptible to errors caused by recrystallization and by non-uniform specimen temperature when large amounts of crystal are undergoing fusion. One problem with this approach is the choice of this arbitrary fraction p .

The maximum slope definition corresponds to the peak temperature of a derivative plot. It corresponds roughly to $p \approx 0.5$, and is subject to the same problems as $T_{m,p}$ at large p .

The definition chosen for this work is the extrapolated temperature $T_{m,E}$ obtained by linearly extrapolating the trace from the point of maximum slope up to the amorphous baseline. $T_{m,E}$ could be considered to be the highest melting temperature that would result if processes leading to the slope reversal were eliminated. Its obvious advantage is the very high resolution obtainable under poor conditions.

Under the worst conditions (noisy baseline, low crystallinity, high heating rate) encountered in this study, the $T_{m,B}$ or $T_{m,p}$ ($p \leq 0.02$) values from a given trace were subject to uncertainties of over 1°C. Under the same conditions, $T_{m,E}$ could be defined to within about 0.1°C.

Differences in the values obtained from these various definitions depended on the experimental conditions, particularly on crystallization temperature T_c and heating rate r . These differences are illustrated in Figure 3, for T_c between -20° and 0°C , at the lowest ($0.2^\circ\text{C min}^{-1}$) and highest (3°C min^{-1}) heating rates used. For clarity, the baseline ($T_{m,B}$) and extrapolated ($T_{m,E}$) values are indicated only by their curves, which were obtained from a significantly larger group of data. The points corresponding to these curves will be presented later in this paper. All samples were crystallized for about 21 h.

The differences between the various melting temperature definitions are fairly uniform except at low crystallization temperatures and low heating rates. Crystal thickening, possibly by melt recrystallization or accelerated

thickening just below the melting point, is significant under these conditions; its effect on points sensitive to the high end of the melting distribution (i.e. $T_{m,B}$ and $T_{m,p}$ at low p) is evident.

RESULTS

A polymer crystal melts at a temperature strongly dependent on the crystallization temperature T_c , but this relation is complicated by other factors, particularly the heating rate r during melting. This is illustrated in Figure 1, which clearly shows the shift to higher temperatures (due to lamellar thickening) at lower heating rates. The greater susceptibility of the $T_{m,B}$ definition to such error is also evident.

Extensive data on the variation of the melting temperature with T_c (-20° to 0°C) and r (0.2° to 3°C min^{-1}) at atmospheric pressure are presented in Figure 4. Crystallization time $t_c \approx 21$ h in each case. As in the rest of the data presented, the extrapolated definition ($T_{m,E}$) of the melting temperature was chosen as standard, but the commonly used baseline definition ($T_{m,B}$) has been included for comparison. The dilatometric data of Kim and Mandelkern³ are also included.

It can be seen from this Figure that data obtained at low T_c and at low heating rate r are more susceptible to thickening during melting. The baseline definition $T_{m,B}$ is also more sensitive to thickening than the extrapolated definition $T_{m,E}$.

Thickening during melting is evident even at $r = 1^\circ\text{C min}^{-1}$, though not as drastic as that at $0.2^\circ\text{C min}^{-1}$. Whether or not thickening occurs at 3°C min^{-1} cannot be concluded from this Figure; it will be seen later that it does occur, though only to a small extent. In any case, all the plots, including the ones at 3°C min^{-1} , show distinct curvature.

The dilatometric data of Kim and Mandelkern³ in Figure 4 are seen to be parallel to the $T_{m,B}$ definition at $0.2^\circ\text{C min}^{-1}$, but about 2°C above it. They have said nothing about sample size or thermal lag calibration; a lag of 2°C in a dilatometer would not be unreasonable. If the highest observable melting temperatures were chosen, as is likely, their data would be compatible with the rest of the Figure.

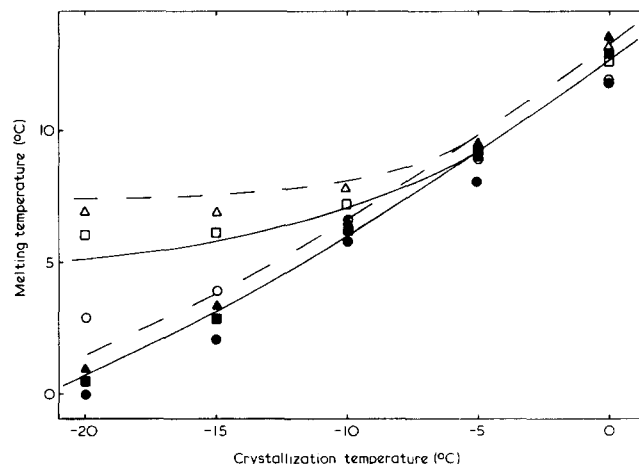


Figure 3 Differences between the various definitions of melting temperature at atmospheric pressure: \blacksquare , \square , $p=0.01$; \bullet , \circ , $p=0.05$; \blacktriangle , \triangle , maximum slope. Heating rates: $0.2^\circ\text{C min}^{-1}$ (open) and 3°C min^{-1} (filled). The curves are from Figure 5

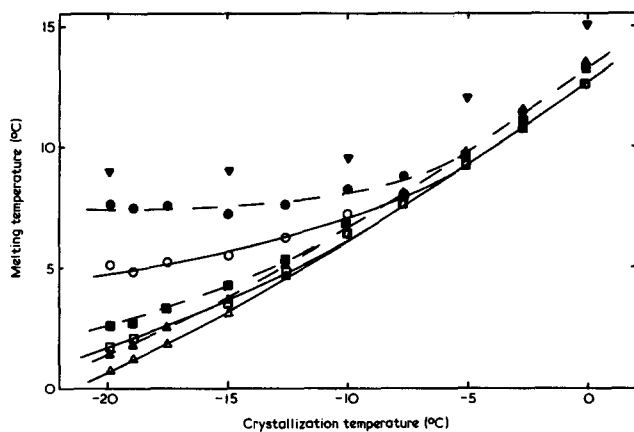


Figure 4 Melting temperature as a function of crystallization temperature at atmospheric pressure. Heating rates: ● ○, 0.2; ■ □, 1; ▲ △, 3°C min⁻¹. Open symbols and full lines represent T_{m,E}. Filled symbols and dashed lines represent T_{m,B}. ▼, data of Kim and Mandelkern³

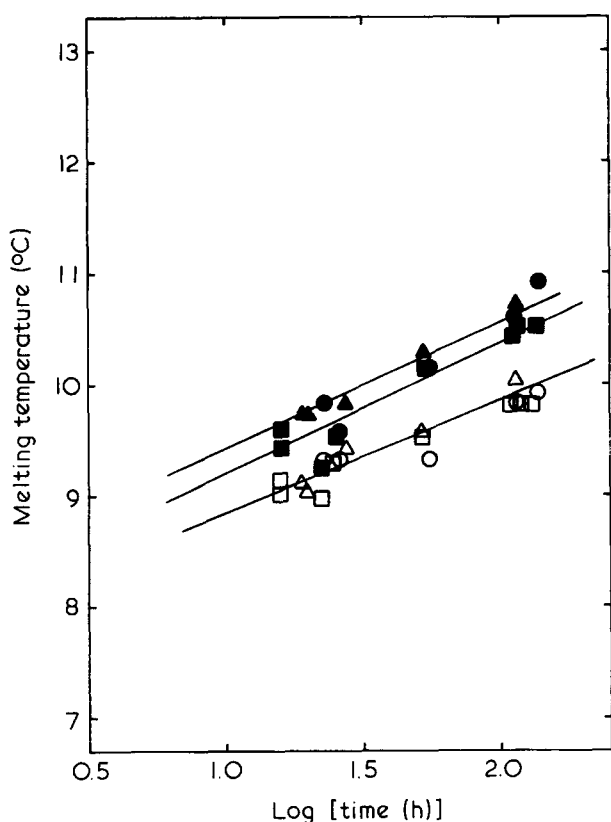


Figure 5 Effect of crystallization time at -5°C on melting temperature. Symbols as in Figure 4

The rate of isothermal thickening at the crystallization temperature T_c , (i.e. the effect of crystallization time t_c) was studied at $T_c = 0, -5, -10, -15$ and -20°C , in terms of the melting temperature. Examples of these data, with three different heating rates and the two melting temperature definitions, are presented in Figure 5 (the remaining data can be found in ref. 4). The time range used was limited at short times by the need for adequate crystallinity to obtain a good melting trace, and at long times by practical considerations.

The melting temperature increased by about 2°C per decade of time at 0°C, but this rate fell to below 0.2°C per decade at -20°C. Heating rate and melting temperature definition appeared to have no effect on this rate.

However, the poor resolution of the baseline definition $T_{m,B}$ showed up clearly as increased scatter in the data; this effect was more pronounced at the lowest crystallization temperatures and the slowest heating rates.

DISCUSSION

The melting temperature T_m of a lamellar polymer crystal is a function of its thickness l , because of the significant contributions of its surfaces to the total free energy. The equilibrium melting temperature T_m° , corresponding to a hypothetical infinitely thick crystal, may be obtained by the direct or indirect extrapolation of T_m data to $l = \infty$.

It can be shown⁶ from thermodynamic considerations that:

$$T_m = T_m^\circ \left(1 - \frac{2\sigma_e}{\Delta h_f l} \right) \quad (1)$$

where σ_e is the end surface free energy and Δh_f is the heat of fusion per unit volume of the crystal. This equation predicts a linear relationship between T_m and $1/l$.

The lamellar thickness l is a function of the crystallization temperature T_c . Rensch *et al.*⁷ have shown, within experimental error, that l for *cis*-polyisoprene is independent of the source (*Hevea*, *Guayule* or *Natsyn*). Consequently, a plot of l versus T_c data for *cis*-polyisoprene from various references was made; this is presented in Figure 6. Interpolation and smoothing of the data were carried out by fitting a second-order polynomial:

$$l = 9.93 + 0.228T_c + 0.297 \times 10^{-2} T_c^2 \quad (2)$$

where l is in nm and T_c is in °C. The correlation coefficient was 98.8% and was not significantly improved by the use of higher orders. The data in Figure 4 were converted, using equation (2), to the plot of T_m versus $1/l$ shown in Figure 7. The departures from linearity are believed to be due entirely to processes involving the finite rate of melting (accelerated thickening and/or melt recrystallization). They are naturally more severe at the lower heating rates.

Excellent linearity for all but the last three points is seen at 3°C min⁻¹. In these three cases, corresponding to the

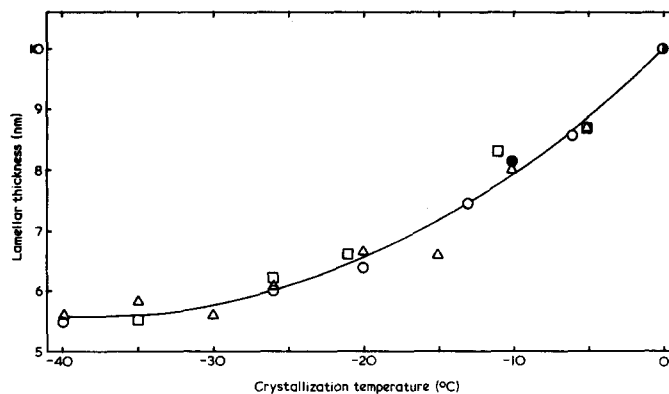


Figure 6 Lamellar thickness versus crystallization temperature for *cis*-polyisoprene at atmospheric pressure. Data from: △, Edwards²; ○, Andrews *et al.*, from Edwards²; ●, Phillips and Edwards⁸; □, Rensch *et al.*⁷. The curve is the regression polynomial of equation (2)

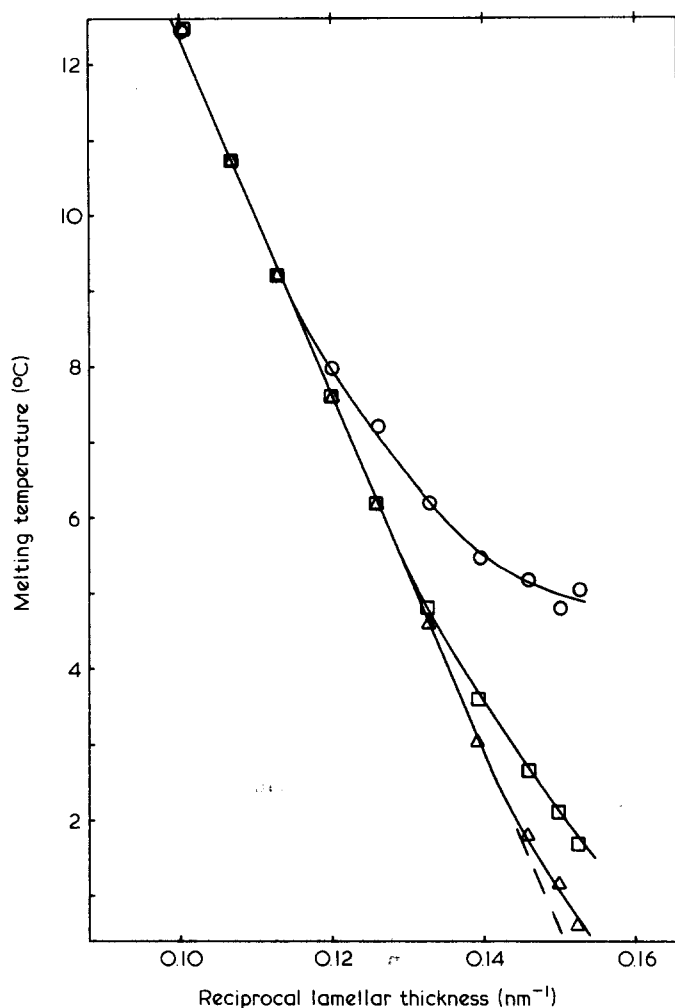


Figure 7 Melting temperature $T_{m,E}$ versus reciprocal lamellar thickness at atmospheric pressure. Symbols as in Figure 4

lowest T_c values, slight thickening during melting had evidently occurred; this thickening increased the melting temperature by about 0.7°C in the worst case. The highest point is also slightly ($\sim 0.2^\circ\text{C}$) above the line. This is probably because the exact crystallization time t_c used in the lamellar thickness data is unknown, and the arbitrary value used ($t_c = 21$ h) may be too high.

A regression line was fitted to all the points at $r = 3^\circ\text{C min}^{-1}$, with the exception of the four thickened points discussed above. This is the straight line of Figure 7. The intercept of this line gave $T_m^\circ = 35.8^\circ\text{C}$. The fold surface free energy σ_e can be obtained from the slope of the line using equation (1), if the heat of fusion Δh_f is known. Taking³ $\Delta h_f = 6.4 \times 10^7 \text{ J m}^{-3}$ gave $\sigma_e = 0.0244 \text{ J m}^{-2}$.

An alternative indirect extrapolation may also be used to obtain T_m° . The initial lamellar thickness l_g^* can be predicted, at a given T_c , from the Lauritzen-Hoffman kinetic theory⁹:

$$l_g^* = \frac{2\sigma_e}{\Delta f} + \left(\frac{kT}{2b\sigma} \right) \left(\frac{4\sigma/a + \Delta f}{(2\sigma/a) + \Delta f} \right) \quad (3)$$

for the reasonable (see ref. 4) case of the parameter $\psi = 0$. Here $\Delta f \approx (\Delta h_f \Delta T / T_m^\circ)$ is the bulk free energy of fusion, $\Delta T = (T_m^\circ - T_c)$ is the undercooling, a is the molecular width, b is the layer thickness and σ is the lateral surface free energy. The last term of equation (3), commonly

referred to as ∂l , is typically quite small. Neglecting it leads⁶ to:

$$T_m \approx T_m^\circ(1 - 1/\gamma) + T_c/\gamma \quad (4)$$

where $\gamma = l/l_g^*$ is assumed to be a constant, independent of T_c . This predicts a linear relationship between T_m and T_c .

In the case of *cis*-polyisoprene, ∂l is found to account for almost 10% of l at low values of T_c , and is hence not properly negligible. It can be taken into account, as shown in ref. 4, by taking:

$$T_m - \{[(K\Delta T) - (K\Delta T)^2]\Delta T/\gamma\}$$

as the ordinate, rather than just T_m . Here:

$$K = \Delta h_f \partial l / 2\sigma_e T_m^\circ$$

Values of γ and T_m° are required in this procedure; they may be obtained iteratively from the slope and intercept of the plot, initiated with T_m as the ordinate, and convergence thereafter is very rapid. Independent values of σ_e and Δh_f are required.

The melting data from Figure 4 at $r = 3^\circ\text{C min}^{-1}$, which undergo very little thickening during melting, are plotted in Figure 8 with and without the ∂l correction described above. A tangent to the uncorrected (upper) curve at high T_c , where it is approximately linear, produces values of $T_m^\circ = 33.8^\circ\text{C}$ and $\gamma = 1.59$ using equation (4). The value of T_m° is 2°C below that obtained from Figure 7, and this value would be even lower if the line were forced through the entire curve.

The corrected (lower) curve was calculated⁴ with $\Delta h_f = 6.4 \times 10^7 \text{ J m}^{-3}$ and $\sigma_e = 0.0244 \text{ J m}^{-2}$ found earlier. The resulting values are $T_m^\circ = 35.2^\circ\text{C}$ and $\gamma = 1.46$, the former comparing very well with $T_m^\circ = 35.8^\circ\text{C}$ from Figure 7.

The ∂l correction has changed the slope (and hence γ) significantly, but the change in T_m° is quite small. In fact, despite the large extrapolation, the change in T_m° is only about a third of the maximum change in T_m . The explanation is that the corrected ∂l value at T_m° , though slightly larger than that in the experimental T_m range, is truly negligible compared to the hypothetical infinite value of l , and the effect of the correction is merely to pivot the curve about the point $T_m = T_c = T_m^\circ$. The uncorrected curve should therefore also have defined this point, except that curvature in the plot prevented an accurate extrapolation. The uncorrected curve, if determined up to sufficiently high temperatures, would in principle define T_m° accurately. In practice, however, at higher crystallization temperatures erroneously high T_m values are obtained due to massive levels of isothermal thickening, brought about by the combination of long crystallization time necessary to get adequate crystallinity and the enhanced thickening rate. This effect is in fact already noticeable at $T_c = 0^\circ\text{C}$, at which point T_m is about 0.2°C higher than the expected curve in Figure 7 as well as in Figure 8.

The relative value of ∂l is also responsible for the fact that the correction is larger at lower temperatures, despite the absolute value of ∂l actually being slightly smaller at this end.

Since the Lauritzen-Hoffman theory⁹ predicts the lamellar thickness at a given T_c , in terms of σ_e , it is possible to obtain an estimate of σ_e from kinetic considerations, in

addition to the thermodynamic value obtained from T_m versus $1/l$ data. The published l versus T_c data presented in Figure 6 will be used in this calculation, the melting data obtained here being used for the sole (but important) purpose of defining T_m° and γ .

It is well established that for many polymers l and ΔT

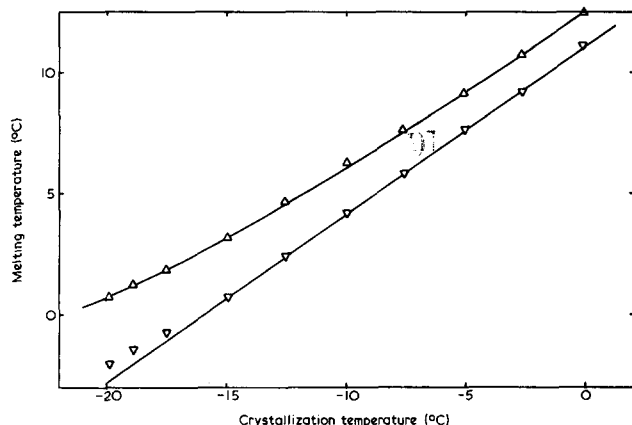


Figure 8 Plot of melting temperature versus crystallization temperature, with (lower line) and without (upper line) the ∂l correction. Atmospheric pressure, heating rate 3°C min^{-1}

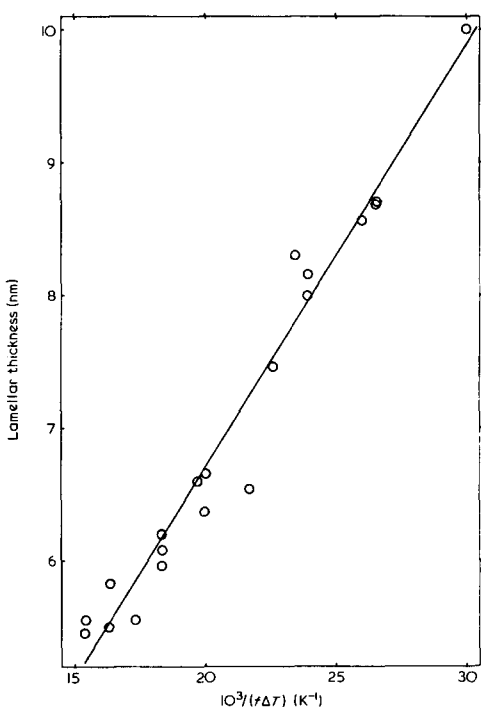


Figure 9 Plot of lamellar thickness against $10^3/(f\Delta T)$ at atmospheric pressure. Data from Figure 11, with $T_m = 35.5^\circ\text{C}$

(hence T_c) can be related, at least for low to moderate undercooling, by the linear empirical equation:

$$l = \frac{c_1}{\Delta T} + c_2 \quad (5)$$

Kinetic theory may be applied⁶ to obtain the parameters c_1 and c_2 in terms of the following collections of fundamental quantities, which may be considered approximately constant over experimentally accessible temperature ranges:

$$c_1 = \frac{2\sigma_{e1}T_m^\circ\gamma}{\Delta h_f} \quad (6)$$

$$c_2 = \frac{2\sigma_{e1}yT_m^\circ\gamma}{\Delta h_f} + \gamma\partial l \quad (7)$$

where σ_{e1} and y represent the temperature dependence of σ_e (see ref. 9):

$$\sigma_e = \sigma_{e1}(1 + y\Delta T) \quad (8)$$

with $\sigma_{e1} \equiv \sigma_e(T_m^\circ)$ and y being a small positive number.

In order for c_2 to be even approximately constant, the parameter ψ in ∂l ^{6,9} must for most materials be very low. This is compatible with the value $\psi = 0$ that we have used in the ∂l correction.

The factor $f = 2T/(T_m^\circ + T)$ was introduced (see ref. 6) to correct for non-linearity in the heat of fusion at large undercoolings. It can be applied here through a minor modification of equation (5):

$$l = \frac{c_1}{f\Delta T} + c_2 \quad (9)$$

Figure 9 shows a plot of l versus $1/(f\Delta T)$, which was drawn using the data of Figure 6. From the slope and intercept respectively, $c_1 = 317.7 \text{ nm K}$ and $c_2 = 0.35 \text{ nm}$ were obtained.

The atmospheric pressure equilibrium melting temperature of cis-polyisoprene has been evaluated earlier in this paper by two different methods to be 35.8° and 35.2°C . An average value of $T_m^\circ = 35.5^\circ\text{C}$ was used in this analysis to define ΔT . Use of either of the two experimental values caused no significant change in the results.

With input values³ of $\Delta h_f = 6.4 \times 10^7 \text{ J m}^{-3}$ and $\gamma = 1.46$ (from the ∂l corrected curve of Figure 8) we obtain $\sigma_{e1} = 0.0239 \text{ J m}^{-2}$, in good agreement with the thermodynamic value (0.0244 J m^{-2}) found from T_m versus $1/l$ data. The values of T_m° and σ_e found by various methods are summarized in Table 1. Throughout this paper, values of

Table 1 Estimates of the equilibrium melting temperature and fold surface free energy of cis-polyisoprene at atmospheric pressure

Technique	Method	Reference	T_m° ($^\circ\text{C}$)	σ_e (J m^{-2})
Turbidimetry*	T_m versus $1/l$	This work*	35.8	0.0244
Turbidimetry	T_m versus T_c (∂l corrected)	This work	35.2	—
Turbidimetry	T_m versus T_c (uncorrected)	This work	33.8	—
TEM	l versus $1/(f\Delta T)$	Various*†	—	0.0239
Dilatometry	T_m versus T_c (uncorrected)	Ref. 5	~39	—

* Lamellar thickness data by transmission electron microscopy from various sources (see Figure 11)

† Our analysis

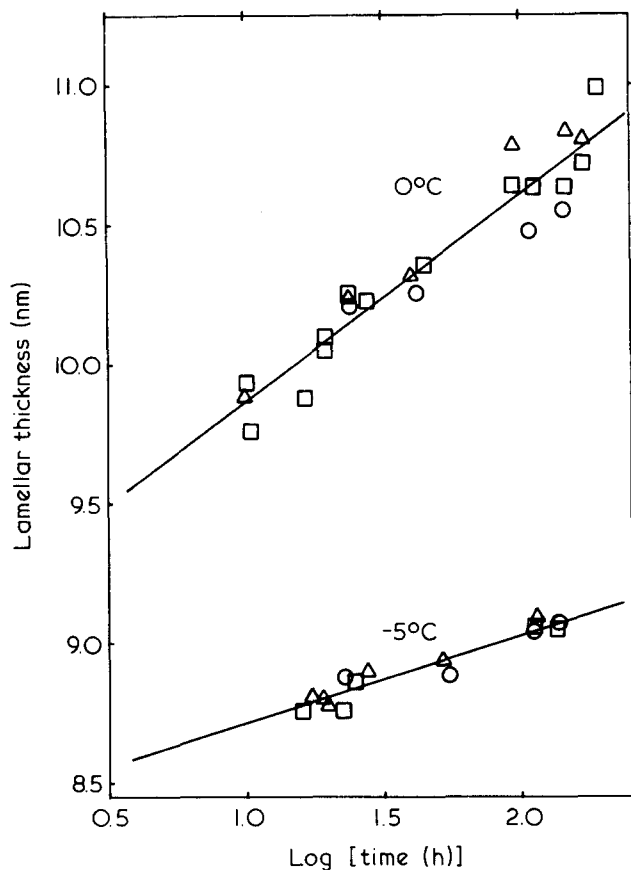


Figure 10 Lamellar thickness as a function of crystallization time at 0°C and -5°C. Symbols as in Figure 5

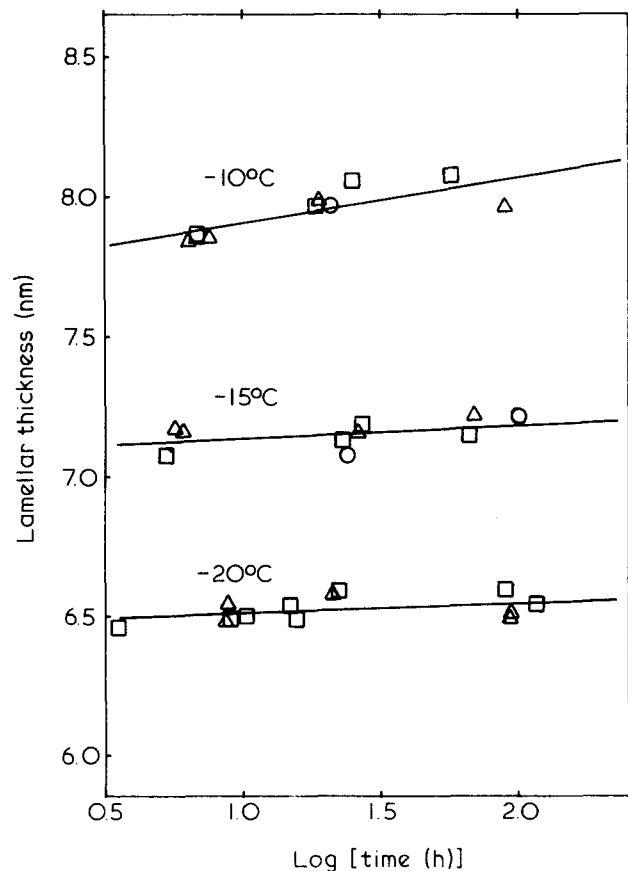


Figure 11 Lamellar thickness as a function of crystallization time at -10°, -15° and -20°C. Symbols as in Figure 5

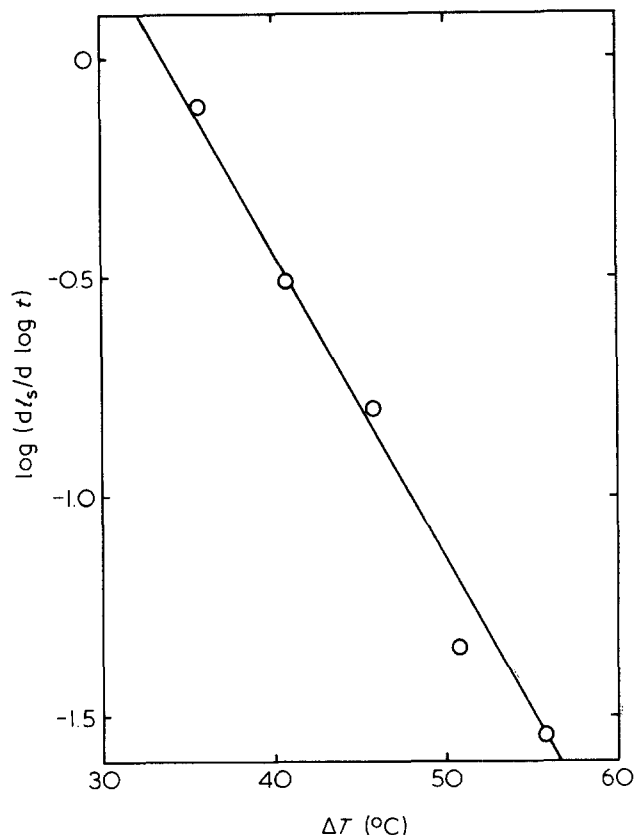


Figure 12 Plot of $\log(dl/d \log t)$ against undercooling ΔT

σ_c reported without any mention of temperature refer to values near T_m° (i.e. σ_{e1}).

Isothermal thickening data may be obtained by combining the T_m versus $\log t_c$ data (e.g. as in Figure 5) with the T_m versus $1/l$ data of Figure 7. The resulting linear plots of l versus $\log t_c$ are presented in Figures 10 and 11. The straight lines in these figures were fitted by least-squares regression. It has been observed empirically (e.g. see ref. 10) that the logarithm of the slope of these lines is proportional to the undercooling ΔT . Such a plot is presented in Figure 12, and is indeed quite linear. The regression line shown corresponds to:

$$\log\left(\frac{dl}{d \log t_c}\right) = 2.325 - 0.0692\Delta T \quad (10)$$

where l is in nm, t is in h and ΔT is in K. When converted to the natural base e , equation (10) can be written as:

$$\frac{dl}{d \ln t_c} = 92.1 \exp(-0.159\Delta T) \quad (11)$$

CONCLUSIONS

Extensive melting data determined by an optical 'turbidimetric' technique, shown to be a reliable and accurate method consistent with other techniques, have been used to determine the equilibrium melting temperature T_m° of cis-polyisoprene at atmospheric pressure. Extrapolation of T_m versus T_c data, subjected to a ∂l correction ($\partial l \approx 0.1l$), gave $T_m^\circ = 35.2^\circ\text{C}$. The alternative extrapolation of T_m versus $1/l$ data gave $T_m^\circ = 35.8^\circ\text{C}$, using published lamellar

thickness data. An average value of $T_m^\circ = 35.5^\circ\text{C}$ is considered to be the best estimate.

The data generated have also been used to evaluate the fold surface free energy σ_e of cis-polyisoprene. T_m versus $1/l$ data gave $\sigma_e = 0.0244 \text{ J m}^{-2}$, while analysis of published l versus $1/(f\Delta T)$ data, using T_m° and γ values obtained in this work, yielded $\sigma_e = 0.0239 \text{ J m}^{-2}$. The value of the heat of fusion Δh_f required in both cases was taken from the literature³.

The resultant value of $\sigma_e \approx 0.024 \text{ J m}^{-2}$ is lower than corresponding values for other polymers listed in Table 6 of ref. 6, lying between 20% and 70% of the σ_e values listed for polymers with C-C chain backbones. For a variety of reasons⁴, the published value³ of Δh_f used in these calculations appears to be too low, providing one possible explanation for the low σ_e .

The work of chain folding⁶ q is found⁴ from σ_e to be about 3 kJ mol^{-1} , which is only 13% of the value for polyethylene and an even smaller fraction of that for the other polymers listed⁶. It is possible that the adjacent re-entry fraction, known to be very low in cis-polyisoprene⁴, is responsible for the low σ_e , and has to be taken into account in calculating q .

ACKNOWLEDGEMENT

This research has been supported by the Polymer Program of the National Science Foundation under grants DMR-78-24696 and DMR-81-06033.

REFERENCES

- 1 Wunderlich, B. 'Macromolecular Physics', Vol. 3, Academic Press, New York, 1980
- 2 Edwards, B. C. *J. Polym. Sci., Polym. Phys. Edn.* 1975, **13**, 1387
- 3 Kim, H.-G. and Mandelkern, L. *J. Polym. Sci., A-2* 1972, **10**, 1125
- 4 Dalal, E. N. Ph.D. Dissertation, University of Utah, 1982
- 5 Weeks, J. J. *J. Res. Natl. Bur. Stand. A* 1963, **67**, 441
- 6 Hoffman, J. D., Davis, G. T. and Lauritzen, J. I., Jr, in 'Treatise on Solid State Chemistry' (Ed. N. B. Hannay), Plenum Press, New York, 1976, Vol. 3, Ch. 7
- 7 Rensch, G. J., Phillips, P. J., Vatansever, A. and Gonzalez, V. A. submitted for publication
- 8 Phillips, P. J. and Edwards, B. C. *J. Polym. Sci., Polym. Phys. Edn.* 1975, **13**, 1819
- 9 Lauritzen, J. I. Jr and Hoffman, J. D. *J. Appl. Phys.* 1973, **44**, 4340
- 10 Sanchez, I. C., Colson, J. P. and Eby, R. K. *J. Appl. Phys.* 1973, **44**, 4332